Dynamic Sound Scattering Investigation of the Dynamics of Sheared Particulate Suspensions

Anatoliy Strybulevych*, Tomohisa Norisuye†, Matthew Hasselfield*, and J. H. Page*

*Department of Physics and Astronomy, University of Manitoba, Winnipeg R3T 2N2, Canada
†Department of Macromolecular Science and Engineering, Graduate School of Science & Technology, Kyoto Institute of Technology, Matsugasaki, Sakyo-ku, Kyoto 606-8585, JAPAN

Abstract. We show how Dynamic Sound Scattering (the acoustical analog of Dynamic Light Scattering) can be used to measure the average velocity profile and the particle velocity variance of neutrally buoyant suspensions in the Couette geometry. The motion of the particles was determined from the temporal autocorrelation function of the scattered field fluctuations in a single speckle spot. In contrast to theories that assume isotropic particle velocity fluctuations, it is shown that "suspension temperature" (defined as the average kinetic energy contained in the particle velocity fluctuations) is a tensor, whose components have different magnitudes. For particle volume fractions up to 0.4, components of the fluctuations parallel to the flow and in the vertical direction are much larger than in the radial direction. For higher concentrations the fluctuation anisotropy decreases.

Keywords: Dynamic sound scattering, Particle dynamics, Suspensions
PACS: 43.20.Fn, 43.35.Yb, 47.57.E-, 47.80.Cb, 82.70.-y

INTRODUCTION

The flow properties of suspensions of solid particles in a liquid have been intensively investigated over the last several decades. The flow of concentrated suspensions often produces particle migration, when an initially uniform distribution of the particles becomes non-uniform. In granular-flow based models (e.g. see [1]), migration of the particles is attributed to gradients in so-called "suspension temperature", defined as the average kinetic energy of particle velocity fluctuations due to interparticle collisions. To explore and understand the fluid dynamics of such suspension under shear, accurate measurement of flow velocities is essential. Such measurements need to be non-intrusive, because any probe inside the suspension may perturb the flow or even change the structure.

Laser Doppler velocimetry (LDV) is the most popular non-intrusive technique [2] to measure velocity profiles. Velocity is obtained from the Doppler shift of laser light scattered by seeding particles moving with the fluid. Particle imaging velocimetry (PIV) may also be used for this purpose. However, concentrated suspensions may be not transparent enough to use LDV and PIV. Nuclear magnetic resonance (NMR) imaging technique [3] can be used for opaque media, but this technique is quite expensive and time consuming.

On the other hand, ultrasound may propagate through optically opaque media. When an ultrasonic wave travels through inhomogeneous media, it gets scattered when the acoustical impedances (product of density and sound velocity) of the particles and surrounding fluid are different. An Ultrasonic Velocity Profiler (UVP) has been developed and successfully used for in-line flow rate and velocity profile measurements [4]. The technique is based on time-domain cross-correlation of ultrasonic speckle signals backscattered by the seeded particles.

Another approach, Dynamic Sound Scattering (DSS) (the acoustical analog of Dynamic Light Scattering) utilizes the temporal autocorrelation function of the scattered field fluctuations in a single speckle spot to measure motion of the particles [5]. The field correlation function is defined as

$$g_1(\tau) = \frac{\int \psi^*(T)\psi(T+\tau)dT}{\int |\psi(T)|^2 dT}, \qquad (1)$$

where $\psi(T)$ is the scattered ultrasonic field measured at time T; its decay results from the change in phase of the scattered ultrasonic field due the particle motion. As discussed by Cowan et al. [5], the field correlation function can be written

$$g_1(\tau) = \langle \exp[-i\Delta\phi_p(\tau)] \rangle = \langle \exp[-i\vec{q}\cdot\Delta\vec{r}_p(\tau)] \rangle, \quad (2)$$

where $\Delta\phi_p(\tau)$ is the phase change of the scattered waves due to the p^{th} particle's motion, $\vec{q} = \vec{k}' - \vec{k} = = 2k\sin(\theta/2)$ is the scattering wave vector, θ is the scattering angle, $\Delta\vec{r}_p(\tau)$ is the change in position of the p^{th} particle during the time interval τ, and $\langle ... \rangle$ denotes time average. Since $\Delta\phi_p(\tau) = \langle \Delta\phi_p(\tau) \rangle + \delta\phi_p(\tau)$, after using a cumulant expansion, the real part of the correlation func-

CP982, *Complex Systems, 5th International Workshop on Complex Systems*
edited by M. Tokuyama, I. Oppenheim, and H. Nishiyama

tion for ballistic particle motion, where $\Delta\vec{r}_p(\tau) = \vec{V}_p\tau$, is

$$g_1(\tau) \simeq \cos[2k\sin(\theta/2)\langle V_{\vec{q}}\rangle\tau] \times \exp[-2k^2\sin^2(\theta/2)\langle\delta V_{\vec{q}}^2\rangle\tau^2]. \quad (3)$$

Thus, the time dependence of the correlation function is determined by the motion of the particles. Since the scattering angle can be controlled by the scattering geometry, and the magnitude of the wave vector k can be measured independently, both the average particle velocity along $\vec{q}$, $\langle V_{\vec{q}}\rangle$, and the variance (or "suspension temperature"), $\langle\delta V^2\rangle = \langle\delta V_{\vec{q}}^2\rangle - \langle V_{\vec{q}}\rangle^2$, can be independently determined by measuring the correlation function.

In this paper, we describe experiments to measure particle dynamics of neutrally buoyant suspensions of uniform glass beads in the Couette geometry using DSS.

MATERIALS AND METHODS

The samples consisted of uniform glass beads (radius 63 $\pm$11 mm, density 2.220 kg/m^3) immersed in a density-matched liquid consisting of a mixture LST (a low viscosity aqueous solution of lithium heteropolytungstates) and water. The measurements were carried out for volume fractions ϕ of 0.2, 0.3, 0.4, 0.45, and 0.5 at a temperature of 27°C. The dynamics were studied under steady shear flow at shear rate,$\dot{\gamma}$, from 0.26 to 8.8 s^{-1} and across the entire gap between the stator and rotor, thereby enabling a complete investigation of the dynamics to be carried out. The experiments were performed using a Couette geometry where the inner cylinder is the rotor, the outer cylinder is the stator, and the sample volume has an inner and outer radius of 54 and 58 mm respectively, corresponding to a gap width, l, of 4 mm. The rotor went straight to the bottom of the cell with a bottom bearing, thereby eliminating any low-shear-rate fluid reservoir at the bottom.

To measure the correlation function in these experiments, the following procedures were followed. The sample cell and ultrasonic transducer were immersed in a water tank, since water is a convenient low-attenuation medium in which the placement of the transducers relative to the cell can be easily controlled. This also allowed precise control of the sample temperature, by regulating the temperature of the water bath. Pulsed experiments were used, in which a regular train of short ultrasonic pulses was sent to the sample, with a repetition time that was generally of order 0.5 - 5 ms depending on the speed of the dynamics. The ultrasonic scattering measurements were performed in reflection mode using a focusing transducer with central frequency of 2.25 MHz, whose orientation relative to the cell was varied. Experiments were carried out for the following orientations (see Fig. 1), so that all three orthogonal components of the

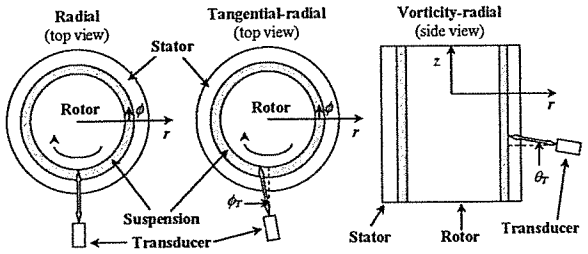

FIGURE 1. Orientations of the transducer for measurements of the three orthogonal components of the particle motions.

particle motions could be measured: radial (beam axis perpendicular to the cell wall), "tangential-radial" (beam axis rotated in the horizontal plane perpendicular to the cylindrical axis (z) with incidence angles ϕ_T = 3, 5 and 7.5°), and "neutral-radial" (beam axis at θ_T = 10 and 15° to the r-axis in the rz or vertical plane). To obtain more complete information during one run, experiments were performed using the gated digitization feature of a GageScope oscilloscope card, which allows the entire scattered ultrasonic waveform as a function of propagation time inside the cell to be captured. The advantage of this approach is more efficient data acquisition, allowing measurements of the particle motions at all depths inside the cell to be measured simultaneously. The data were then saved to the computer hard drive and the process repeated up to 20 times, depending on the statistics desired. The correlation function was calculated numerically using a FFT approach from the digitized data.

RESULTS AND DISCUSSION

An example of the scattered waveforms for a 30 % suspension of glass beads in LST/water, recorded using the GageScope for many repetitions of the input pulse, is shown in Fig. 2. The transducer was oriented in the "tangential-radial" direction and the mean shear rate was 4.145 s^{-1}. The figure shows an image plot of the wave field, with the y-axis representing distance from the stator determined from the pulse propagation time. In the image plot, white indicates wave crests and black represents the wave troughs. Near the stator, the wave crests are almost tangential to the fluctuation time axis, indicating that the phase of the scattered waves barely changes, corresponding to very slow motion of the beads, while deeper into the cell, the wave crests tilt markedly downwards, indicating increasing rapid motion. Note that the white and black bands are not continuous in the image plot, a signature of fluctuations in the particle velocities. This behavior is also captured in Fig. 3, which shows the scattered wave field versus fluctuation time T at three

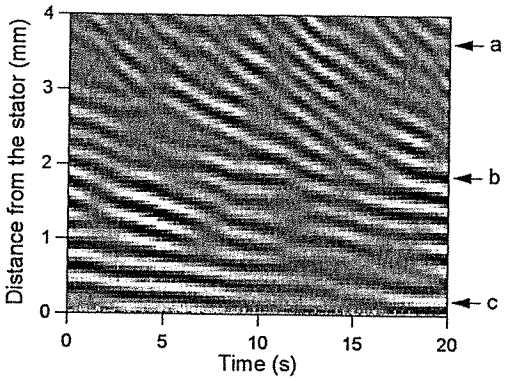

FIGURE 2. Image plot of the scattered wave field as a function of distance inside the cell and fluctuation time T.

depths inside the cell, labeled a, b, and c, and indicated by arrows in Fig. 2. It is evident that the field fluctuations are more rapid near the rotor than the stator, and are neither perfectly regular in T nor completely random. The corresponding field autocorrelation functions at these depths are shown in Fig. 4, where the data have been averaged over 10 sequences similar to those plotted in Fig. 3 to improve the statistics. As the propagation time of the pulse and the depth inside the cell increases, the autocorrelation function decays more rapidly, confirming that the motion of the beads is also more rapid. The shape of the correlation function, a Gaussian decay modulated by a sinusoidally varying term, indicates that the bead motion is one of particles moving predominantly in one direction, with substantial fluctuations about this average velocity. This shape is exactly what is predicted for this type of motion (see Eq. (4)). By fitting Eq. (4) to the measured autocorrelation functions, both the average velocity $\langle V_{\vec{q}} \rangle$ and the velocity variance $\langle \delta V^2 \rangle$ can be accurately determined along the direction given by the scattering wave vector $\vec{q}$.

Figure 5 compares the field autocorrelation functions for three orientations of the transducer: radial, "neutral-radial" with $\theta_T = 15°$, and "tangential-radial" with $\phi_T = 5°$. The correlation functions were measured in the middle of the gap, for the 30% glass bead suspension sheared at $\dot{\gamma} = 4.145\,\mathrm{s}^{-1}$. It is clear from the figure that only in the "tangential-radial" direction is there a negative dip in the correlation function, indicating only in the tangential direction parallel to the flow is the average velocity of the beads non-zero. The solid curves in the figure are fits of Eq. (4) to the data, with $\langle V_{\vec{q}} \rangle = 0$ for both the radial and neutral directions. Excellent fits are obtained, giving reliable measurements of the average particle velocity in the "tangential-radial" direction and the velocity variance along all three measurement directions.

To extract the components of the velocity and variance along the radial, tangential and neutral directions, it is necessary to account for the refraction of ultrasound at the cylindrical cell walls and for the propagation of not only the longitudinal waves in the wall but also shear waves generated by mode conversion at the interface. Since a focusing transducer is used, the input beam contains a range of angles, and so it is also necessary to average over these angles. For a given direction we measure

$$2k\langle \vec{V} \rangle_{meas} = P_r \langle V_r \rangle + P_\phi \langle V_\phi \rangle + P_z \langle V_z \rangle \quad \text{and} \quad (4)$$

$$4k^2 \langle (\delta V^2)_{meas} = Q_r \langle \delta V_r^2 \rangle + Q_\phi \langle \delta V_\phi^2 \rangle + Q_z \langle \delta V_z^2 \rangle \quad (5)$$

where r, ϕ and z refer to the cylindrical polar coordinates of the cylindrical cell, $\langle \vec{V} \rangle_{meas}$ and $\langle (\delta V^2 \rangle_{meas}$ are the fitted values from the correlation functions, assuming backscattering. The parameters $[P_r, P_\phi, P_z]$ and $[Q_r, Q_\phi, Q_z]$ were then calculated for a transducer of specified size, position and orientation, for a cylindrical cell of given acoustic properties and dimensions, and for a sample of known acoustic properties (which depend on particle concentration).

Figure 6 shows the variation $\langle V \rangle$ and $\langle \delta V^2 \rangle$ with distance inside the cell for the 30% suspension obtained from different transducer orientations. The figure shows that the average velocity across a Couette gap at all three orientations is linear, and good agreement between the predictions and experiments are found. Despite the quite wide gap, the shear profile is linear in the cell for the shear rates used in experiments, and there is no evidence of slippage of the suspension near the stator or rotor, since the average particle velocity varied from zero at the stator to a value equal to the wall velocity at the rotor.

The dependence of "suspension temperature" components on volume fraction for four different shear rates is presented in Fig. 7. In comparing the components in

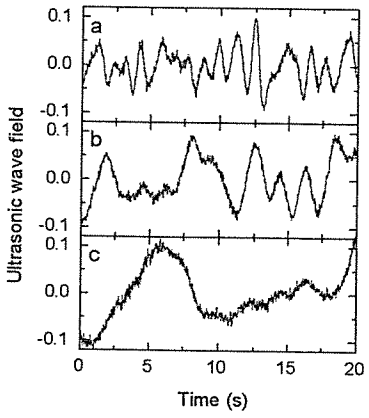

FIGURE 3. Field fluctuations as a function of time at the depths a, b, and c indicated by the arrows in Fig. 2.

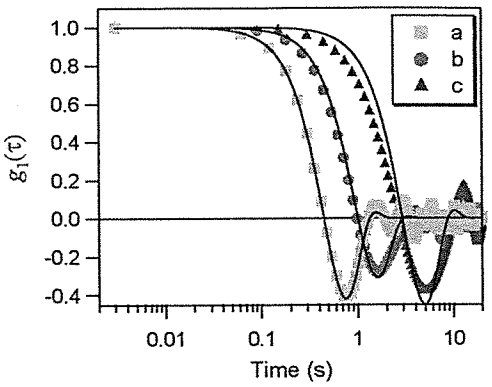

FIGURE 4. Corresponding field autocorrelation functions for the data shown in Fig. 3.

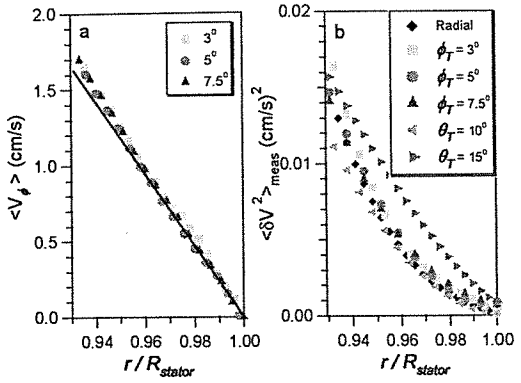

FIGURE 6. Comparison of (a) average velocity and (b) variances profiles for different transducer orientations with theoretical predictions (solid line) for a 30% dispersion.

these four graphs, it is clear that the tangential component at particle volume fractions up to 0.4 is the largest, followed by the vertical and then the radial components. For higher concentrations the fluctuation anisotropy decreases. It is also apparent that each of the three components varies differently with particle concentration. The radial components is almost independent of particle concentration; it appears to increase slightly and then drops significantly for highest concentration. The tangential component monotonically decreases and the vertical component has a maximum at volume fraction of 0.3. Similar behavior was observed by Shapley et al. [6].

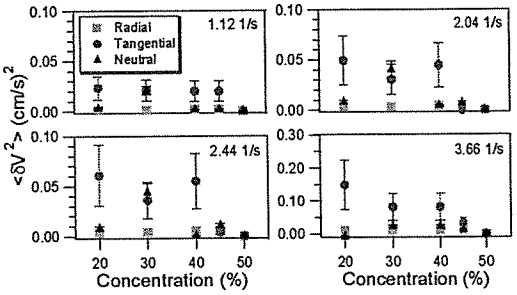

FIGURE 7. Components of the variance as function of particle volume fraction for different shear rate.

CONCLUSIONS

In this paper, we demonstrate that Dynamic Sound Scattering is a powerful new technique for investigating the dynamics of sheared particulate suspensions. It was found that the average particle velocity increases linearly with distance from the stator, indicating that the average motion conforms to simple shear flow. The fluctuations in the particle velocities are quite large, indicating that the particles are not confined to streamlines but continue to fluctuate substantially during steady flow. For particle volume fractions up to 0.4, components of the fluctuations parallel to the flow and in the vertical direction are much larger than in the radial direction. For higher concentrations the fluctuation anisotropy decreases.

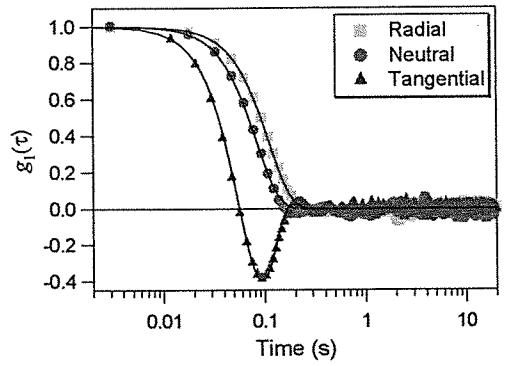

FIGURE 5. Temporal field autocorrelation functions of the scattered fields for the three transducer orientations indicated in the legend.

ACKNOWLEDGMENTS

Support of this research by the Canadian Space Agency is gratefully acknowledged.

REFERENCES

1. P. R. Nott, and J. F. Brady, *J. Fluid Mech.* **275**, 157–199 (1994).

2. F. Durst, A. Melling, and J. Whitelaw, *Principles and Practice of Laser-Doppler Anemometry*, Academic, New York, 1981.
3. A. W. Chow, S. W. Sinton, and J. H. Iwamiya, *Phys. Fluids* **6**, 2561–201 (1994).
4. Y. Takeda, *Exp. Therm. Fluid Sci.* **10**, 444–453 (1995).
5. M. Cowan, J. Page, and D. Weitz, *Phys. Rev. Lett.* **85**, 453–456 (2000).
6. N. Shapley, R. Brown, and R. Armstrong, *J. Rheol.* **48**, 255–279 (2004).